Sagittal focusing of synchrotron radiation diffracted on the walls of a longitudinal hole drilled into a single-crystal monochromator

N. Artemiev,[a]* J. Hrdý,[a] S. Peredkov,[b] A. Artemev,[c] A. Freund[d] and R. Tucoulou[d]

[a]Institute of Physics, Academy of Sciences of the Czech Republic, Na Slovance 2, 18221 Praha 8, Czech Republic, [b]MAX-Lab, Lund University, PO Box 118, S 22100 Lund, Sweden, [c]Russian Research Centre, Kurchatov Institute, Kurchatov Sq. 1, 123182 Moscow, Russia, and [d]ESRF, BP 220, 38043 Grenoble, France. E-mail: artemiev@fzu.cz

A very simple method of sagittal focusing of X-ray synchrotron radiation is presented. A special ray-tracing program which utilizes the diffraction–refraction effect is developed. It is demonstrated both by ray-tracing simulations and by an experiment whereby a reasonably good sagittal concentration of 8 keV synchrotron radiation may be achieved by diffraction on the walls of a cylindrical hole drilled into an Si crystal. The holes were drilled parallel to the (111) planes and their diameter, 1 mm, was chosen so that the focusing distance fits the geometrical arrangement of beamline BM5 at the ESRF. Two such crystals have been used in a dispersive and non-dispersive arrangement. The better result was achieved using the dispersive arrangement. The intensity at the centre of the focus is increased by five times with respect to unfocused radiation. Excellent agreement exists between the ray-tracing simulations and experimental results.

Keywords: ray tracing; X-ray optics; X-ray crystal monochromators; inclined diffraction; diffraction–refraction effect; focusing.

1. Introduction

The utilization of refraction phenomena for focusing of X-ray synchrotron radiation is now well established. The compound refractive lens (Snigirev *et al.*, 1996) is an analogue to the classical refractive lens in visible optics. It employs relatively simple instrumentation and works well for hard radiation. For longer wavelengths, however, absorption in the lens material may deteriorate the intensity gain due to focusing. To avoid this drawback, rather sophisticated schemes have been suggested (Lengeler *et al.*, 1999; Piestrup *et al.*, 2000) which substantially reduce the absorption, but the manufacturing of such lenses is non-trivial.

An alternative way of focusing synchrotron radiation based on refraction was proposed by Hrdý (1998). The main idea is to utilize the refraction phenomenon occurring during Bragg diffraction (diffraction–refraction effect). It was shown that the radiation diffracted from a longitudinal groove with parabolic profile machined into a single-crystal monochromator is sagittally concentrated (focused). In this case, the grooved crystal plays the role of both X-ray monochromator and sagittally focusing lens. There are no losses due to absorption as in the case of the compound refractive lens. At the same time it was shown that it is better to use the dispersive arrangement of such grooved crystals.

Sagittal focusing based on this idea was first experimentally demonstrated at the National Synchrotron Light Source at Brookhaven National Laboratory (Hrdý & Siddons, 1999), where 15 keV radiation was successfully focused at a distance of 4.5 m after successive diffraction on four grooved-crystal surfaces arranged in a $(-++-)$ position. A grooved single crystal is a relatively simple device but the production of the parabolic groove of given parameters requires a specially profiled tool. This is expensive and the tool can be used only once (or a few times in the best case). In this paper we show that in some cases a relatively good sagittal concentration of synchrotron radiation can be achieved by using a cylindrically shaped groove instead of a parabolic groove, and that such a sagittally focusing monochromator may be realised by a cylindrical hole drilled into a single crystal parallel to the diffracting planes. In other words, the hole plays the role of a channel with inclined walls.

2. Ray tracing

The use of the diffraction–refraction effect calls for substantial improvements to existing programs or the development of new ray-tracing programs. In order to check the focusing ability of different optical systems based on the refraction phenomenon occurring during Bragg diffraction, a special ray-tracing program has been developed.

The program allows us to create one-, two- and three-dimensional sources of different real- and phase-space distributions. The optical element is a perfect crystal, which can have a working surface of any shape. The crystallographic planes are not distorted but a groove is machined into the surface of the crystal. The number of optical elements is unlimited. Each optical element may have a working surface of different shape, such as a parabola, ellipse, cylinder or plane, inclined and/or asymmetrical with respect to the diffracting planes, as well as any other profile. This is input as an ASCII file. The program calculates sagittal and meridional deviations of a ray on an inclined and/or an asymmetrical surface of the optical element. The mathematical model of the calculations is based on the dynamical theory of diffraction. In order to obtain the intensity distribution in the beam, a virtual screen can be inserted at any place in the optical system. It is also possible to obtain the footprint of the incident radiation on each optical element. An output data file contains three real-space and two phase-space coordinates for each ray.

Four ray-tracing calculations corresponding to four possible crystal arrangements are presented in Fig. 1. The corresponding optical schemes are shown above each ray-tracing plot. All of the examples were calculated under the same conditions, which fit the layout of beamline BM5, *i.e.* a source-to-crystal distance of 40 m and a crystal-to-focal-plane distance of no larger than 2 m. The photon energy was 8 keV and the diameter of the hole was 1 mm. In each ray-tracing plot, black dots represent the ray tracing without taking into account the refraction phenomenon occurring during Bragg diffraction on an inclined surface, while red dots show the 'real case' where X-rays diffracted on the walls of the hole are deflected from the plane of diffraction in the sagittal direction.

Fig. 1(*a*) represents the focusing ability of a set of two crystals with cylindrical holes arranged in an antiparallel position. The X-ray beam is reflected twice inside each hole. The focal distance is 2 m. Fig. 1(*b*) shows the ray-tracing results for the same crystal arrangement but in this case the hole is longer, the X-ray beam is reflected four times inside each hole, and the focal distance is only 1 m. Fig. 1(*c*) presents sagittal focusing after six reflections and in this case the focusing distance is 1.37 m. The ray-tracing results for a parallel arrangement of such crystals are shown in Fig. 1(*d*). Here again the incident beam undergoes only two reflections inside each hole and the focal distance is 1.5 m. It is seen that in this case the aberrations are larger.

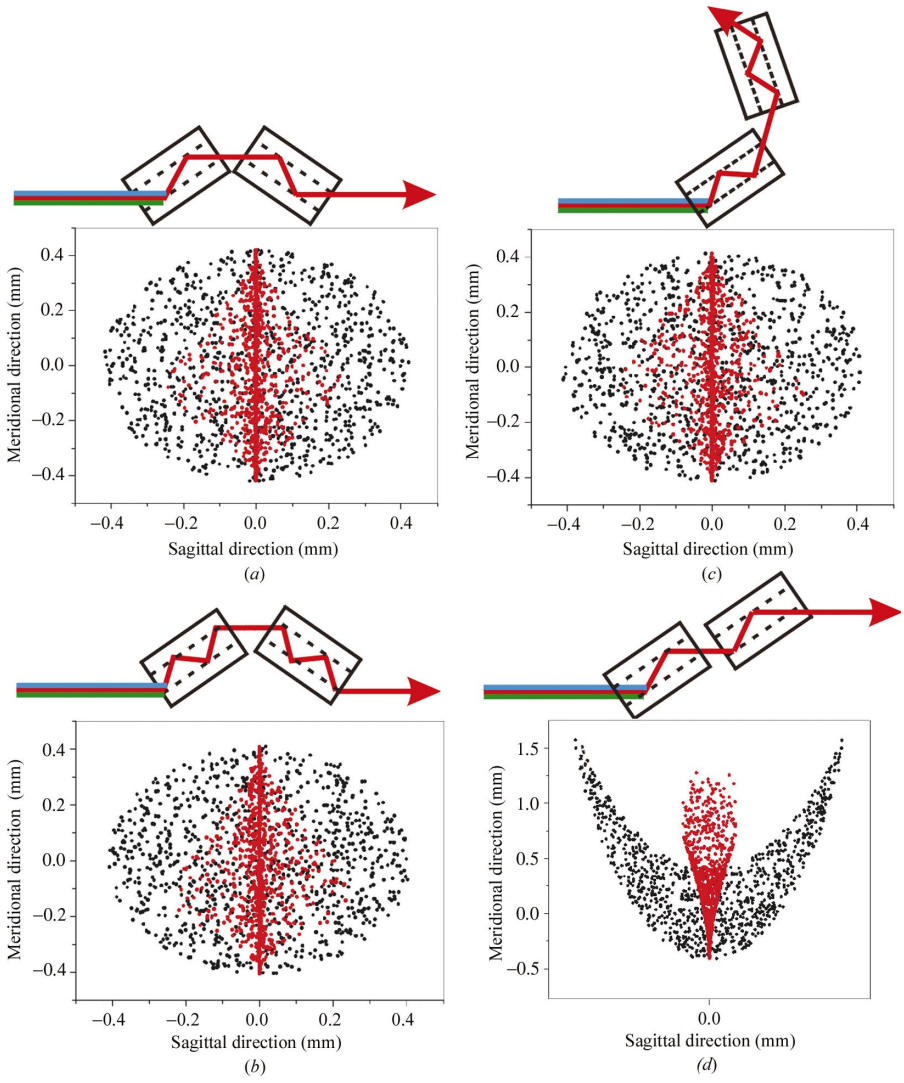

Figure 1
Ray-tracing examples of different crystal arrangements (see text).

3. Experiment description

A photograph of a crystal with a hole is shown in Fig. 2. A channel with plane working surfaces on the right-hand side of the crystal is cut to simplify the alignment procedure and to compare intensities of focused and unfocused radiation.

In order to utilize the small vertical source size (~80 μm) and to achieve maximal flexibility in the arrangement and adjustment of the equipment of beamline BM5, the crystals were oriented in such a way that a beam was focused in the vertical direction. A top view of the experimental layout is shown in Fig. 3.

The diameter of the hole in each crystal is 1 mm. This value is taken from the condition that the focal distance for 8–10 keV incidence radiation must fit the layout of beamline BM5, where the experiment was carried out.

Unfortunately, we could not use the standard double-crystal monochromator of beamline BM5 because of its dispersion in the vertical direction. Therefore, in order to decrease the heat load on the first sample crystal and to avoid fast damage of the detectors, a

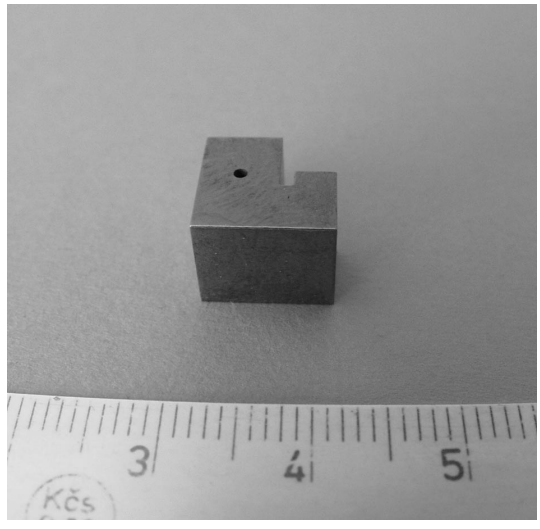

Figure 2
A crystal with a cylindrical hole.

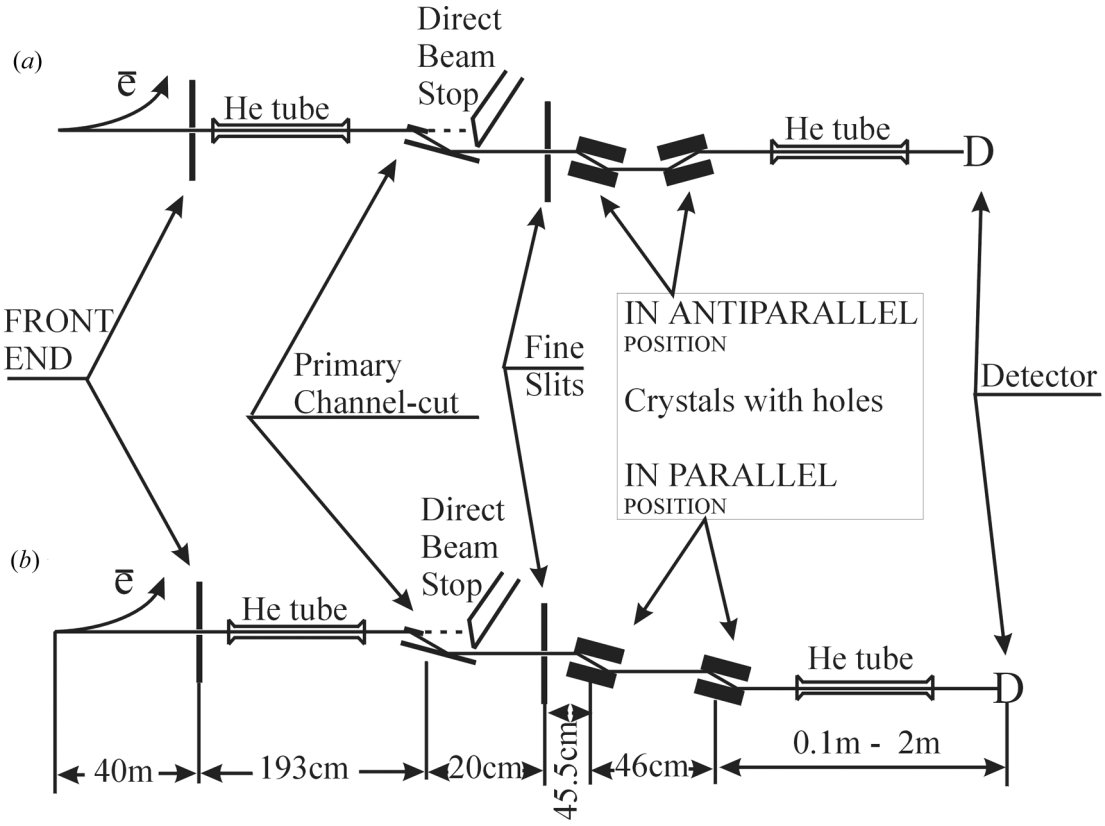

Figure 3
Top view of the experimental layout for (*a*) antiparallel and (*b*) parallel crystals arrangements.

primary channel-cut Si(111) crystal was installed on the first goniometer head in such a way that its dispersion plane was horizontal.

Slits (1 mm × 1 mm) were installed on the same goniometer head, 20.5 cm downstream of the primary channel crystal.

The first sample crystal with a hole was mounted on the second and most versatile goniometer head, which has all degrees of freedom. The second sample crystal and the detector were mounted on the third goniometer head. The distance between the sample crystals was 0.46 m, which is the minimal distance between the axes of the second and third goniometer heads. The detector was placed at two different distances, 0.1 m and 2 m downstream from the last crystal with a hole. A high-resolution Kodak X-ray film was used as a detector. In order that the incident beam could be directed into the holes or into the channels to obtain a focused or unfocused beam spot, the crystals were moved perpendicular to the axis of the incident beam in the horizontal direction.

4. Results and discussions

Experimental photographs of the focal spots, their processed plots and corresponding ray-tracing images for antiparallel and parallel arrangements of the sample crystals are shown in Figs. 4 and 5, respectively. The distance from the second sample crystal to the X-ray films was 2 m.

The upper pairs of diagrams in Figs. 4 and 5 present the experimental images of the focal spots and corresponding ray-tracing scatter plots, both shown on the same scale. Beneath these figures the corresponding three-dimensional plots of the intensity distribution and the contour plots are depicted. The beams diffracted in the channels, which are cut into the sides of the sample crystals (see Fig. 2), are not focused. Experimental images of the unfocused beams are not shown. In comparison with the intensity in the focuses, the intensity of the unfocused beam is shown in the left-hand corners of the three-dimensional plots and on the upper parts of the corresponding contour plots. On the three-dimensional and contour plots of the ray-tracing results, the shapes of the unfocused beam spots correspond to the ray tracing of the same optical system, *i.e.* crystals with holes, but without taking into account the diffraction–refraction effect. In the case of the antiparallel arrangement of the crystals, the profile and the intensity distribution of the beam are the same as if the beam has been diffracted in the channels. For the parallel arrangement of the crystals, however, the shape of the beam spot is completely different, but the intensity distribution along the beam spot is similar to that of an unfocused beam.

It can be clearly seen that aberrations are much larger in the case of a parallel (non-dispersive) arrangement of the crystals. First of all, this is related to the shape of the working surfaces of the crystals and the corresponding optical paths of the geometrical rays through the optical system. Also, for the parallel arrangement the smearing effect accompanying inclined Bragg diffraction (Artemiev *et al.*, 2000) is increased by a factor which is equal to the number of reflections, while in the case of an antiparallel (dispersive) arrangement this effect is practically cancelled out, or is at least less noticeable. Despite the fact that the intensity distribution in the case of the parallel arrangement of the crystals is broader, the peak intensity is 17% higher than in the case of the antiparallel arrangement. The full width

at half-maximum of the intensity distribution in the focal spot is 169 μm for the antiparallel arrangement and 218 μm for the parallel arrangement of the sample crystals.

Aberrations of such an optical system increase with increasing demagnification factor. This is because the exact parabolic profile of the focusing elements is approximated by a cylinder. In our case the demagnification is about 20, which is quite high. The aberrations of this particular optical scheme are quite noticeable, even in the case of the antiparallel arrangement of the crystals. This is because the distance between the crystals (0.46 m) is not negligible when compared with the focal distance (2 m).

Fig. 6 shows photographs of the radiation diffracted inside a hole, and the corresponding ray-tracing simulations are shown for two different distances, 0.46 m and 2 m. The crescent-like image shown in Fig. 6(*a*) was taken at 10 cm from the crystal. It obviously represents the topography of the crystal surface inside the hole. The two faint horizontal lines above and below the main sharp image are traces of the third harmonic. A photograph of the radiation diffracted by the same crystal, which was taken at a distance of 2 m from the crystal, is shown in Fig. 6(*b*). It consists of two partially overlapping images. The inner horseshoe-like image corresponds to the footprint of the first harmonic, squeezed in the vertical direction due to the refraction effect. The outer crescent-like image, which has practically the same shape as the image in Fig. 6(*a*), is the footprint of the third harmonic for which the refraction effect is much smaller.

The ray-tracing simulations show that at short distances from the crystal the spatial deviation of rays due to refraction is barely observable, and the images of radiation diffracted inside a hole

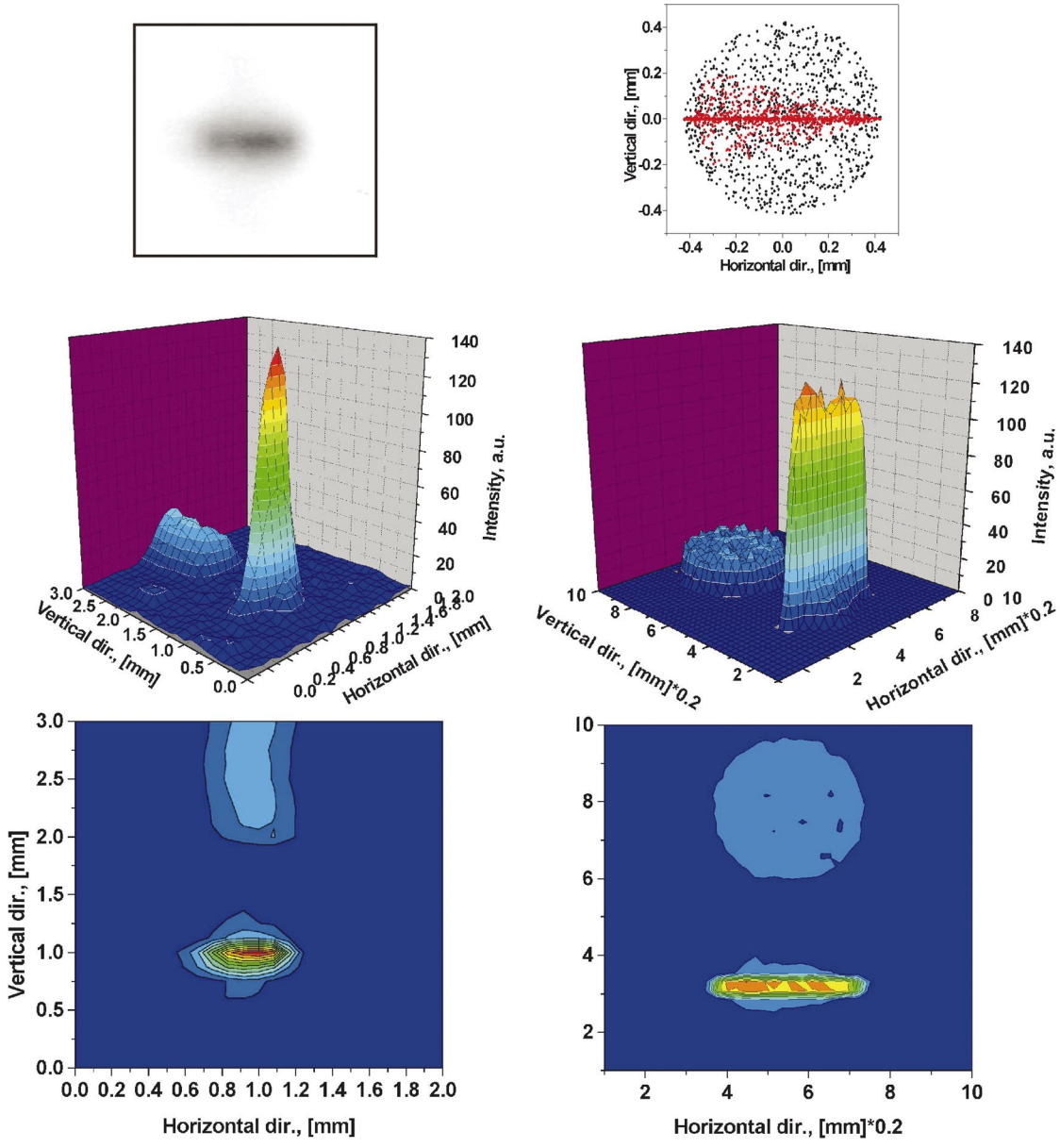

Figure 4
Antiparallel (dispersive) crystals arrangement. Left-hand side: experimental image of the focal spot, three-dimensional plot of the measured intensity, and contour plot. Right-hand side: scatter plot of the ray-tracing simulation for the exact parameters of the experimental layout, three-dimensional plot of the intensity, and contour plot.

calculated with (red dots) and without (black dots) taking into account this refraction effect practically coincide (Fig. 6*c*). This is not true for the image taken at a relatively long distance from the crystal. Fig. 6(*d*) clearly shows the difference between the images calculated with and without taking into account the refraction effect.

The small difference in the shapes of the experimental photographs and corresponding ray-tracing images is explained below.

The ray tracing is based on an approximate but very simple description of inclined Bragg diffraction on the basis of the dynamical theory of diffraction, which is a good approximation up to an inclination angle of ~84°. According to this simplified solution, the sagittal deviation δ of a ray diffracted on an inclined surface is proportional to the tangent of the inclination angle β,

$$\delta = K \tan \beta,$$

where $K = 1.256 \times 10^{-3} \lambda$ [nm] d [nm] for Si (Hrdý, 1998). The validity of this simple formula has been experimentally checked and its limitation has been determined from exact calculations (Artemiev *et al.*, 2000).

In the experiment the size of the incoming beam was 1 mm × 1 mm which meant that those parts of the walls of the holes with an inclination angle higher than 84° were also illuminated.

It would not make sense to improve the ray-tracing code such that it was able to calculate precisely the sagittal deviation up to an inclination of 90° because aberrations of such an optical element would be dominant.

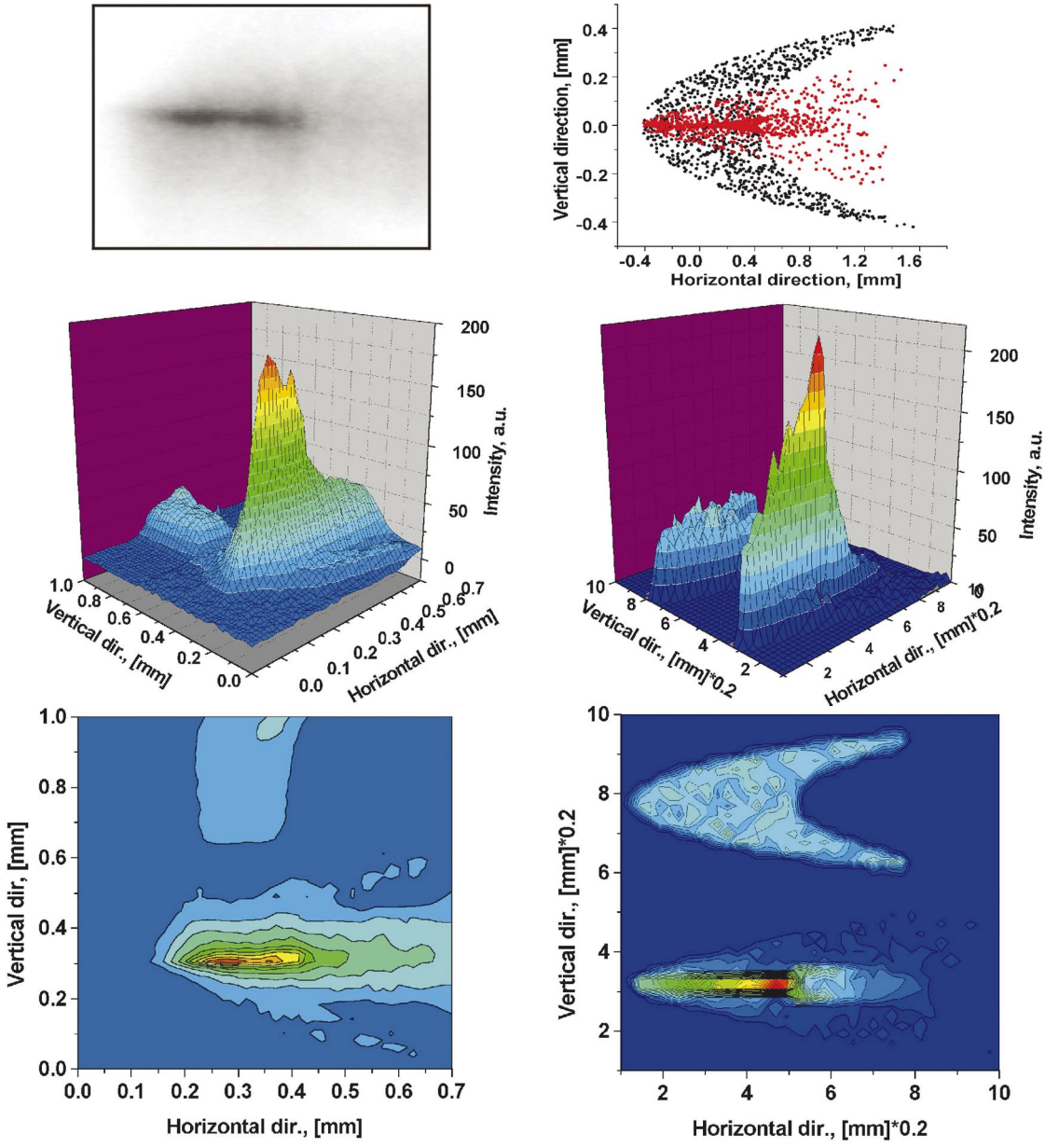

Figure 5
Parallel (non-dispersive) crystals arrangement. Left-hand side: experimental image of the focal spot, three-dimensional plot of the measured intensity, and contour plot. Right-hand side: scatter plot of the ray-tracing simulation of the exact parameters of the experimental layout, three-dimensional plot of the calculated intensity, and the corresponding contour plot.

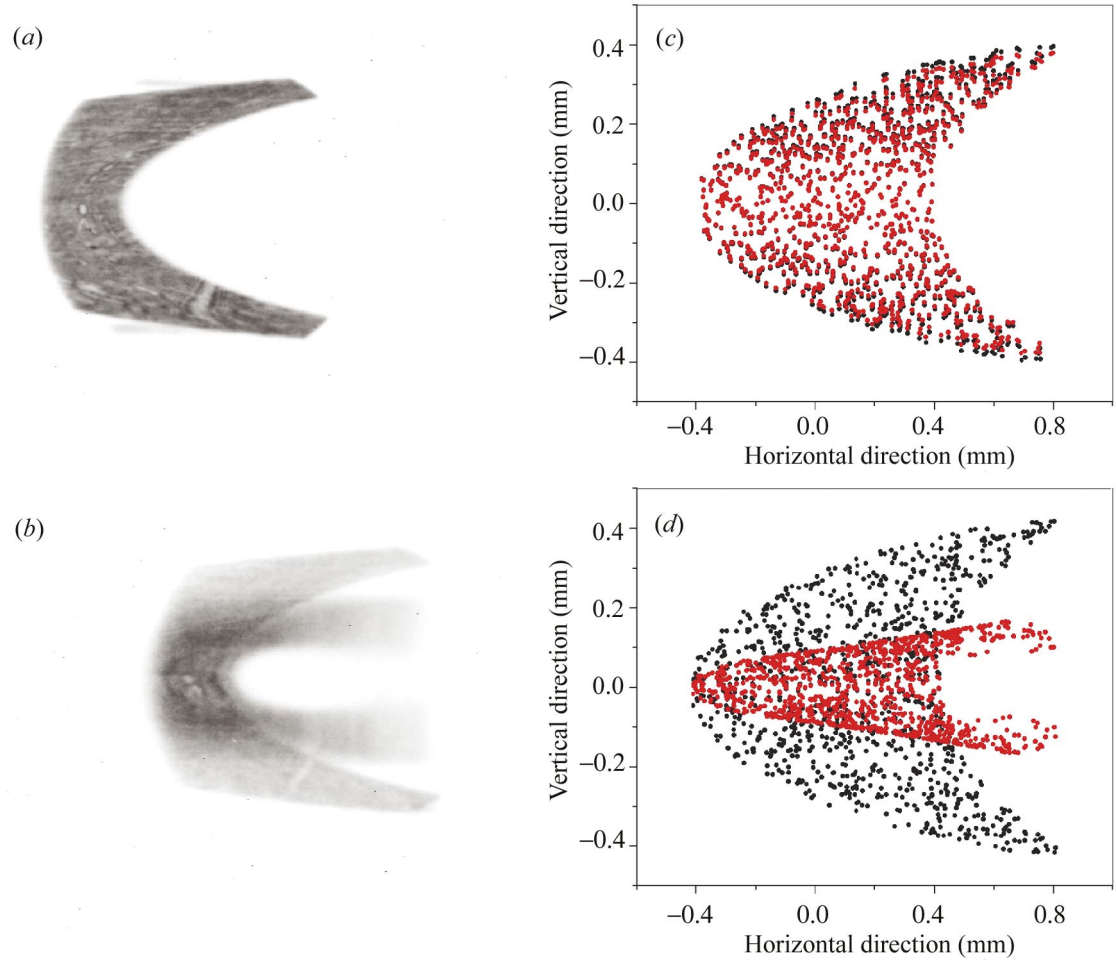

Figure 6
Photographs of radiation diffracted inside a hole taken at 10 cm (*a*) and 2 m (*b*) from the crystal, and the corresponding ray-tracing plots (*c* and *d*).

Also, the ray-tracing model does not take into account the real entrance aperture of the hole. In our ray-tracing calculations, an incident beam of circular cross section is consequently diffracted on separate crystals with half-cylindrical longitudinal grooves.

5. Conclusions

The experimental results show that the real intensity in the focal spot is five times higher than in a spot without focusing. This is quite a reasonable result if one takes into account the large aberration of such a scheme when a hole is completely filled with radiation. Moreover, holes were simply drilled and etched without any special treatment and their cross sections are not perfect circles.

One of the main advantages of this focusing method is its low sensitivity to the working surface quality in comparison with focusing mirrors. Relatively large deviations of inclination angle δ from its ideal value, *i.e.* errors of profile of the focusing surface, lead to relatively small deviations of the diffracted rays from their perfect directions. Moreover, one of the main advantages of this focusing method is its low sensitivity to the working surface profile in comparison with focusing mirrors. Relatively large deviations of inclination angle δ from its ideal value, *i.e.* figure errors, lead to rather small deviations of the diffracted rays from their perfect directions.

Another positive aspect of this focusing method is related to the roughness of the working surface. In the case of X-ray mirrors, for example, roughness plays a dominant role in the reflectivity, and their surfaces must be polished to an ultimate accuracy, *i.e.* the r.m.s. surface roughness should be about a few tens of a nanometer or even better, while in our case roughness on a micrometre scale does not diminish the reflectivity but creates only a weak blurring of the focal spot.

Moreover, as is well known, aberrations increase sharply with decreasing incidence angle. In comparison with a focusing mirror, where the incident beam makes an angle of only a fraction of a degree with the surface, angles for our scheme are of the order of a few degrees. This makes our focusing elements less sensitive to the quality of the working surface. A large angle of incidence realises another important advantage, namely that of the small size of the focusing elements, which in our case is not more than 10 cm.

According to the ray-tracing results (Figs. 4 and 5), the maximum gain which could be achieved in this case is about 7. It is worth noting that in the case of a hole with larger diameter and longer focusing distance, *i.e.* smaller demagnification factor, the aberrations are much smaller and the gain in the focal spot is much higher. Also, the aberrations of such an optical scheme could be decreased if the distance between the crystals is much smaller than the distance between source and optical system and the focal distance.

The advantage of this scheme is obvious: focusing and monochromatization of X-ray synchrotron radiation is performed by the same optical elements without the need of bending crystals.

We would like to express our thanks to Dr Irina Snigireva who helped us to perform preliminary processing of experimental images in the microscopic laboratory at the ESRF. We would also like to thank Ing. F. Franc for his help and assistance in the image processing. This work was partially supported by MPO, Czech Republic, contract No. PZ-CH/22, and GAAV, Czech Republic, contract A1010104/01.

References

Artemiev, N., Busetto, E., Hrdý, J., Pacherova, O., Snigirev, A. & Suvorov, A. (2000). *J. Synchrotron Rad.* **7**, 382–385.
Hrdý, J. (1998). *J. Synchrotron Rad.* **5**, 1206–1210.
Hrdý, J. & Siddons, P. (1999). *J. Synchrotron Rad.* **6**, 973–978.
Lengeler, B., Shroer, C., Tummler, J., Benner, B., Richwin, M., Snigirev, A., Snigireva, I. & Drakopoulos, M. (1999). *J. Synchrotron Rad.* **6**, 1153–1167.
Piestrup, M., Cremer, J., Beguiristain, H., Gary, C. & Pantell, R. (2000). *Rev. Sci. Instrum.* **71**, 4375–4379.
Snigirev, A., Kohn, V., Snigireva, I. & Lengler, B. (1996). *Nature (London)*, **384**, 49–51.